Journal for ImmunoTherapy of Cancer

Intratumoral administration of CD1c (BDCA-1)$^+$ and CD141 (BDCA-3)$^+$ myeloid dendritic cells in combination with talimogene laherparepvec in immune checkpoint blockade refractory advanced melanoma patients: a phase I clinical trial

Julia Katharina Schwarze ,[1] Jens Tijtgat,[1] Gil Awada ,[1] Louise Cras,[2] Angela Vasaturo,[3] Christopher Bagnall,[3] Ramses Forsyth,[2] Inès Dufait,[4] Sandra Tuyaerts,[1] Ivan Van Riet,[5] Bart Neyns [1]

To cite: Schwarze JK, Tijtgat J, Awada G, *et al*. Intratumoral administration of CD1c (BDCA-1)$^+$ and CD141 (BDCA-3)$^+$ myeloid dendritic cells in combination with talimogene laherparepvec in immune checkpoint blockade refractory advanced melanoma patients: a phase I clinical trial. *Journal for ImmunoTherapy of Cancer* 2022;**10**:e005141. doi:10.1136/jitc-2022-005141

► Additional supplemental material is published online only. To view, please visit the journal online (http://dx.doi.org/10.1136/jitc-2022-005141).

Accepted 01 September 2022

For numbered affiliations see end of article.

Correspondence to
Dr Julia Katharina Schwarze; JuliaKatharina.Schwarze@uzbrussel.be

ABSTRACT

Background Intratumoral (IT) myeloid dendritic cells (myDCs) play a pivotal role in initiating antitumor immune responses and relicensing of anti-tumor cytotoxic T lymphocytes within the tumor microenvironment. Talimogene laherparepvec (T-VEC) induces immunogenic cell death, thereby providing maturation signals and enhancing the release of tumor antigens that can be captured and processed by CD1c (BDCA-1)$^+$ / CD141 (BDCA-3)$^+$ myDCs, in order to reinvigorate the cancer-immunity cycle.

Methods In this phase I trial, patients with advanced melanoma who failed standard therapy were eligible for IT injections of ≥1 non-visceral metastases with T-VEC on day 1 followed by IT injection of CD1c (BDCA-1)$^+$ myDCs +/- CD141 (BDCA-3)$^+$ myDCs on day 2. T-VEC injections were repeated on day 21 and every 14 days thereafter. The number of IT administered CD1c (BDCA-1)$^+$ myDCs was escalated from 0.5×10^6, to 1×10^6, to a maximum of 10×10^6 cells in three sequential cohorts. In cohort 4, all isolated CD1c (BDCA-1)$^+$ / CD141 (BDCA-3)$^+$ myDCs were used for IT injection. Primary objectives were safety and feasibility. Repetitive biopsies of treated lesions were performed.

Results In total, 13 patients were enrolled (cohort 1 n=2; cohort 2 n=2; cohort 3 n=3; cohort 4 n=6). Patients received a median of 6 (range 3–8) T-VEC injections. The treatment was safe with most frequent adverse events being fatigue (n=11 (85%)), fever (n=8 (62%)), and chills/influenza-like symptoms (n=6 (46%)). Nine (69%) and four patients (31%), respectively, experienced pain or redness at the injection-site. Clinical responses were documented in injected and non-injected lesions. Two patients (cohort 3) who previously progressed on anti-PD-1 therapy (and one patient also on anti-CTLA-4 therapy) developed a durable, pathologically confirmed complete response that is ongoing at 33 and 35 months following initiation of study treatment. One additional patient treated (cohort 4) had an unconfirmed partial response as best response; two additional patients had a mixed response (with durable complete responses of some injected and non-injected lesions). On-treatment biopsies revealed a strong infiltration by inflammatory cells in regressing lesions.

Conclusions IT coinjection of autologous CD1c (BDCA-1)$^+$ +/- CD141 (BDCA-3)$^+$ myDCs with T-VEC is feasible, tolerable and resulted in encouraging early signs of antitumor activity in immune checkpoint inhibitor-refractory melanoma patients.

Trial registration number NCT03747744.

BACKGROUND

The treatment landscape for patients with metastatic melanoma has changed fundamentally after the introduction of therapeutic monoclonal antibodies directed against the immune checkpoint receptors cytotoxic T-lymphocyte-associated protein 4 (anti-CTLA-4; eg, ipilimumab), and programmed cell death protein 1 (anti-PD-1; eg, nivolumab), and mitogen-activated protein kinase pathway-targeted therapy (restricted to patients with a $BRAF^{V600}$ mutant melanoma).[1–5] Notwithstanding the significant improvement in survival obtained with these therapeutic options, only a minority of patients (19%–36%) will remain free from progression 5 years after initiating therapy, and most patients will require additional treatment options.[1 6 7]

Cancer cells can be recognized by the immune system, a process that is referred to as the 'cancer-immunity cycle'.[8–12] Recent findings have shown that myeloid dendritic

cells (myDCs) play an essential role in the initiation of antigen-specific antitumor immunity.[11 13]

It has been shown in mouse models that myDCs are essential for priming antitumor T-cell responses, with cDC1 (Batf3-dependent CD103$^+$/CD141$^+$ DCs) mediating CD8$^+$ cytotoxic T lymphocytes (CTL) and cDC2 (CD1c$^+$) mediating CD4$^+$ T-cell responses.[14] In order to accomplish this, myDCs need to process tumor antigens and mature (including upregulation of C-C chemokine receptor type 7), migrate to tumor-draining lymph nodes and present tumor antigens to T cells. Moreover, myDCs are essential in 're-licensing' antitumor T lymphocytes to eradicate tumor cells within the tumor microenvironment (TME).[11] Animal models indicate that exclusion of myDCs from the TME is a tumor-intrinsic mechanism of immune evasion.[15] One of the mechanisms that have been identified to play a role in the exclusion of Batf3-expressing myDCs from the TME is the activation of the oncogenic WNT/β-catenin pathway leading to downregulation of the production of chemokines necessary to attract myDCs from the blood.[13 16 17] Absence of myDCs at the invasive margin and within metastases has been correlated with defective CTL activation, thereby allowing metastases to escape antitumor immune responses.[18] Data from The Cancer Genome Atlas (TCGA) indicate a correlation between myDCs and improved survival in various tumor types.[11 12 19] Interestingly, the presence of intratumoral myDCs was more strongly correlated with T-cell infiltration into tumors than neoantigen load in 266 melanomas from TCGA.[20] Mouse models have shown that natural killer (NK) cells form conjugates with DCs in the TME, and that their genetic or cellular ablation demonstrated their importance in the positive regulation of DC abundance in tumor through production of FMS-like tyrosine kinase 3 ligand, defining a TME that is responsive to checkpoint blockade.[21] Of interest, there is evidence that anti-PD-1 efficacy depends on a DC-T-cell licensing loop that is driven by IL-12 and IFN-γ, confirming a central role of DCs in checkpoint blockade.[22]

Myeloid DCs are also present in the blood and have recently been classified according to their surface markers and function.[15 23] Clinical grade immunomagnetic bead isolation of myDCs from peripheral blood mononuclear cells (PBMC) has recently become feasible for CD1c (BDCA-1)$^+$ myDCs, CD141 (BDCA-3)$^+$ myDCs, and BDCA-4$^+$ plasmacytoid DCs (pDCs).[24] While CD14$^+$ CD1c (BDCA-1)$^+$ myDCs have an immunosuppressive phenotype, CD1c (BDCA-1)$^+$ myDCs that do not express CD14 are capable of mediating immune responses induced by immunogenic cancer cell death.[25] Appropriately activated human CD1c (BDCA-1)$^+$ myDCs secrete high levels of interleukin-12 (IL-12) and potently prime CTL responses.[26] Optimal maturation with secretion of IFN-γ as well as the orientation of stimulated T lymphocytes toward a Th1 phenotype ex vivo is achieved following Toll-like receptor stimulation.[27] Immunogenicity and objective tumor responses have been reported in clinical trials exploring the therapeutic value of antigen-loaded CD1c (BDCA-1)$^+$ myDC-derived vaccines for patients with melanoma and prostate cancer.[28–30] Early experience with intratumoral administration of CD1c (BDCA-1)$^+$ myDCs in patients with advanced solid tumors was feasible and safe in combination with intratumorally administered ipilimumab and avelumab plus low dose intravenous nivolumab, and resulted in promising antitumor efficacy.[31]

Talimogene laherparepvec (T-VEC; Imlygic®; Amgen) is the first oncolytic viral therapy approved for use in the clinical setting which is based on a modified herpes simplex virus type 1.[32] T-VEC is designed to selectively replicate in and lyse tumor cells, thereby promoting regional and systemic antitumor immunity.[33–35] Local production of granulocyte macrophage colony-stimulating factor (GM-CSF) leading to recruitment of antigen-presenting cells is achieved by expression of the inserted gene encoding for GM-CSF. T-VEC induces immunogenic tumor cell killing, release of tumor antigens, type I interferons and danger signals, thereby inducing host antitumor immunity.[36] Its approval for the treatment of patients with stage IIIB/C and stage IV-M1a melanoma is based on the phase III OPTiM trial that indicated durable response rates compared with intratumoral injection of GM-CSF.[34 37] Combined with pembrolizumab, T-VEC has been associated with clinical benefit in advanced melanoma patients in a phase I study, as assessed by overall response rates (ORR).[38] Nevertheless, antitumor efficacy has not been confirmed in a randomized phase III trial that failed to meet its primary endpoint of improved progression-free survival.[39]

We hypothesize that intratumorally administered CD1c (BDCA-1)$^+$ myDC with or without CD141 (BDCA-3)$^+$ myDCs in a T-VEC inflamed TME will capture tumor antigens in vivo and through cross-presentation of these antigens coordinate an effective antitumor T-cell response. In this phase I study, we investigate the safety and feasibility of intralesional administration of autologous, non-manipulated CD1c (BDCA-1)$^+$ myDCs with or without CD141 (BDCA-3)$^+$ myDCs plus T-VEC in patients with advanced melanoma who previously progressed on standard therapy including immune checkpoint blockade (ICB).

METHODS

Patients

Patients with unresectable, advanced melanoma (American Joint Committee on Cancer (AJCC) 8th edition stage III or stage IV) who progressed on standard-of-care therapies including at least one anti-PD-1-containing regimen and presented with injectable (sub)cutaneous or lymph node metastases were eligible. Other key inclusion criteria included: age ≥18 years; Eastern Cooperative Oncology Group (ECOG) performance status of 0 or 1; normal hematological, liver, and renal function tests; and negative serological tests for HIV, syphilis, hepatitis B and C. Exclusion criteria included leptomeningeal

metastases, untreated/symptomatic central nervous system metastases, systemic corticosteroid treatment, a history of autoimmune diseases, and the need for permanent therapeutic anticoagulation.

Study design and treatment

This trial is a single-center, open-label phase I trial. Patients were treated in three cohorts with escalating doses of autologous, non-substantially manipulated CD1c (BDCA-1)$^+$ myDCs. Patients in cohorts 1, 2, and 3 were treated with 0.5×10^6, 1×10^6, and 10×10^6 CD1c (BDCA-1)$^+$ myDCs, respectively. Treatment at a next dose level was allowed if no high grade myDC-related adverse events (AE) were observed at the previous dose level. Patients in cohort 4 were treated with a CD1c (BDCA-1)$^+$ / CD141 (BDCA-3)$^+$ myDC co-product; all isolated CD1c (BDCA-1)$^+$ / CD141 (BDCA-3)$^+$ myDCs were injected intratumorally (no dose escalation). On day 1, patients first underwent a leukapheresis, and then were treated with intratumoral injections of selected lesions with T-VEC (10^6 plaque-forming units (PFU)/mL, maximum volume of 4 mL). Approximately 24 hours later (day 2), the same lesions as treated on day 1 were injected with the predefined dose of CD1c (BDCA-1)$^+$ myDCs (cohorts 1–3) or CD1c (BDCA-1)$^+$ / CD141 (BDCA-3)$^+$ myDCs (cohort 4). Patients were then treated with T-VEC (10^8 PFU/mL, maximum volume of 4 mL) on day 21 and every 14 days thereafter until disappearance, progressive disease (PD), unacceptable toxicity, or patient's withdrawal of consent. The injected volume per lesion ranged from 0.1 mL for lesions <0.5 cm to 4.0 mL for lesions >5 cm in longest diameter according to standard dosing guidelines for T-VEC.[40]

Leukapheresis and isolation of myDCs

PBMCs were obtained by leukapheresis of 15 L of blood using the Cobe Spectra device (Terumo Europe, Leuven, Belgium). For the first seven patients (cohorts 1–3), CD1c (BDCA-1)$^+$ myDC were isolated using the CliniMACS Plus platform (Miltenyi Biotec, Bergisch Gladbach, Germany). First, CD14$^+$ and CD19$^+$ cells were depleted with the CliniMACS CD14 and CD19 Reagents followed by positive selection of CD1c (BDCA-1)$^+$ myDCs by using CliniMACS CD1c (BDCA-1)-biotin and CliniMACS Anti-Biotin Reagent (Miltenyi). The isolated CD1c (BDCA-1)$^+$ myDC fraction was concentrated by centrifugation and resuspended in phosphate-buffered saline/EDTA (Miltenyi) containing 0.5% human albumin to obtain a cell suspension at the concentration (cells/mL) desired for clinical administration. For patients in cohort 4, a combined selection of CD1c (BDCA-1)$^+$ myDCs and CD141 (BDCA-3)$^+$ myDCs was performed with the same CliniMACS reagents as mentioned above with the addition of CliniMACS CD141 (BDCA-3) Microbeads. Both the depletion and positive selection step for this cohort were performed using the CliniMACS Prodigy platform (Miltenyi). The final CD1c (BDCA-1)$^+$ myDC and CD141 (BDCA-3)$^+$ myDCs suspensions were concentrated and prepared for infusion as described for cohorts 1–3.

Purity of the isolated CD1c (BDCA-1)$^+$ / CD141 (BDCA-3)$^+$ myDC co-product was analyzed by flow cytometry (MACS Quant Analyzer 10, Miltenyi) using the following monoclonal antibodies: CD14 FITC, CD45 PE, CD123 APC-Vio770, FcεR VioBlue, CD1c PE-Vio770 and CD141 APC with 7-AAD for dead cell exclusion (all antibodies from Miltenyi). The purity of the myDC preparations was analyzed by flow cytometry. The gating strategy for the CD1c (BDCA-1)$^+$ myDCs has previously been described by our group. For the combined CD1c (BDCA-1)$^+$ / CD141 (BDCA-3)$^+$ myDC product, cells were stained with fluorescently-labeled antibodies for CD45, 7-AAD (viability marker), CD14, CD141 (BDCA-3), CD123, CD1c (BDCA-1) and FcεR. Cells were first gated based on FSC/SSC characteristics, followed by gating on CD45$^+$ cells. Next, dead cells were excluded, followed by the exclusion of CD14$^+$ cells. On this gate, CD141$^+$ cells were identified as CD141 (BDCA-3)$^+$ myDC. On the CD141- gate, CD123-FcεR$^+$ CD1c$^+$ cells were identified as CD1c (BDCA-1)$^+$ myDCs. A representative plot of the gating strategy for CD1c (BDCA-1)$^+$ / CD141 (BDCA-3)$^+$ myDC isolation procedure is provided in online supplemental figure S1. Predefined release criteria were a cell viability of >50% and a purity of >85% for CD1c (BDCA-1)$^+$ myDCs and a viability of >50% and a purity of >50% for CD1c (BDCA-1)$^+$/CD141 (BDCA-3)$^+$ myDCs.

Assessment of tumor response and toxicity

Tumor assessment was performed by whole-body fluorodeoxyglucose (^{18}F) positron emission tomography/computed tomography (^{18F}FDG-PET/CT) at baseline and every 12 weeks thereafter. ORR were evaluated using the modified Response Evaluation Criteria in Solid Tumors for immunotherapy (iRECIST).

Safety was assessed on a continuous basis until 30 days after the last study treatment administration. AEs were classified for type, frequency, and severity according to the National Cancer Institute Common Terminology Criteria for Adverse Events (V.5.0). The database was locked on March 10, 2021.

Tumor biopsies, immunohistochemistry, and immunofluorescence

Repetitive biopsies of injected lesions were performed, when feasible. Biopsies were collected using a 18G Vacu-Cut needle (BD BARD) or by punch-biopsy. HE staining and immunohistochemistry (IHC) for SOX10, CD3, CD8, and PD-L1 were performed on formalin-fixed, paraffin-embedded (FFPE) tissue blocks of all biopsies. CD3 2GV6 Ventana (Roche, Basel, Switzerland), CD8 SP57 (Roche), SOX10 SP267 Cell Marque (Roche), and PD-L1 22c3 (Agilent, California, USA) antibodies were used. Evaluation for immunoreactivity was performed by a pathologist according to a semiquantitative scoring system. The Panoramic SCAN II BF was used for scanning representative tissue slides.

On biopsies of interest multiplexed immunofluorescence (mIF) was performed with the Immuno8 FixVUE

panel (Ultivue, Cambridge, Massachusetts, USA), containing antibody-conjugates against CD3, CD4, CD8, CD68, FoxP3, PD-1, PD-L1, and panCK/SOX10, as described by Vasaturo and Galon.[41] DAPI was used for nuclear counterstain. Staining was conducted on a Leica Biosystems BOND RX autostainer. A tissue sample of a tonsil was used as a run positive control. Image acquisition was achieved using the Zeiss Axio Scan.Z1 slide scanner. Images were analyzed using HALO v3.0 software (Indica Labs, USA). The same image analysis algorithm was used were used for all biopsies.

Gene expression profiling

Total RNA was isolated from FFPE-pretreated tumor biopsies. Initially, tumor samples from seven patients were selected; total RNA extraction was sufficient for nine tumor samples from five patients. Gene expression profiling (GEP) of 770 genes was performed using the NanoString PanCancer IO 360 Panel (NanoString Technologies) according to the manufacturer's instructions. Released tags were quantified in a standard nCounter analysis system (NanoString). Biological signatures and scores based on the GEP were provided by NanoString Technologies.

Statistical analysis

Descriptive statistics are provided for baseline demographics, treatment disposition and safety as appropriate. Summary statistics, including median and range, are provided for continuous variables; frequency and percentage are provided for categorical and binary variables.

'All signatures' results table for GEP provides the fold-change values for each signature used to generate a forest plot. The table reports a signature name, variable (when applicable), time point comparison, Log_2 transformed fold change, 95% lower confidence of the mean limit, 95% upper confidence of the mean limit, Student's t-test distribution score, unadjusted significance (p value), and significance adjusted for multiple tests. Spaghetti plots were generated to display the individual sample scores for a single signature (t-test). Unadjusted p values are provided for each signature.

RESULTS

Patient characteristics

Between September 24, 2018 and August 9, 2020, 14 patients were screened and 13 patients were enrolled and initiated study treatment (a disposition of patients enrolled in this trial is provided in figure 1). In cohort 1 and cohort 2, two patients each were enrolled; in cohort 3, three patients were enrolled; in cohort 4, six patients were enrolled. Nine patients (69%) were female, and the median age was 64 years (range 31–81). All patients had an ECOG performance status of 0–1 at the time of enrolment, except for one patient in cohort 1 with ECOG 2 (a waiver for enrolment was given to this patient). One patient (8%) had unresectable AJCC eighth edition stage III melanoma; all other patients had stage IV melanoma. Enrolled patients were pretreated with a median of three prior lines of therapy. Nine (69%) patients received three or more prior lines of systemic therapy. All patients were previously treated with anti-PD-1 checkpoint inhibition

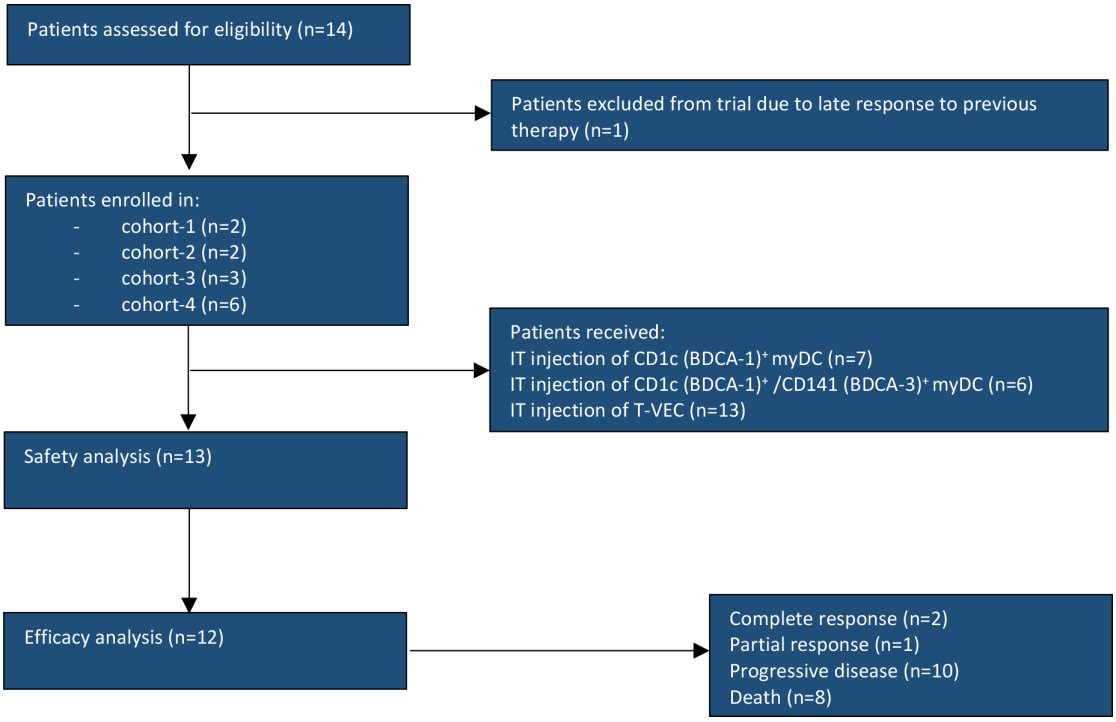

Figure 1 Disposition of patients enrolled in the study.

Table 1 Baseline demographics and disease characteristics (N=13)

Characteristic		Patients, no (%)
Age, median (range) in years		64 (31–81)
Sex	Female	9 (69)
	Male	4 (31)
ECOG	0	10 (77)
	1	2 (15)
	2	1 (8)
Stage	IIIC	1 (8)
	IV-M1a	3 (23)
	IV-M1b	1 (8)
	IV-M1c	6 (46)
	IV-M1d	2 (15)
BRAFV600	Mutation	5 (39)
	Wild type	8 (62)
Prior lines of systemic therapy	Median (range)	3 (2–9)
	1 or 2	4 (31)
	>2	9 (69)
Type of prior treatment	Anti-PD-1 monotherapy	13 (100)
	Anti-CTLA-4 monotherapy	12 (92)
	Anti-PD-1/-CTLA-4 combination	1 (8)
	BRAF-/MEK-inhibition	5 (39)
	Cytotoxic therapy	6 (46)
Injected lesion at baseline	No of myDC-injected lesions, median (range)	2 (1–15)

Tumor stage was determined according to the American Joint Committee on Cancer TNM 8th edition. Cytotoxic therapy included DTIC, temozolomide.
CTLA-4, cytotoxic T-lymphocyte-associated protein 4; ECOG, Eastern Cooperative Oncology Group; myDC, myeloid dendritic cells; PD-1, programmed death-1.

(pembrolizumab or nivolumab), and 12 patients (92%) were treated with anti-CTLA-4 checkpoint blockade. All $BRAF^{V600}$ mutant patients (n=5; 39%) failed previous treatment with BRAF-/MEK-inhibitors. Six patients (46%) also failed one or more lines of chemotherapy. Baseline patient characteristics and demographics, and disease characteristics are listed in table 1.

Isolation and characterization of myDCs

All patients successfully underwent a leukapheresis leading to the collection of CD1c (BDCA-1)$^+$ cells, with a yield varying among from 18.2 to 104.8 × 10^6 cells (all cohorts), except for one outlier (in cohort 1) with a lower yield of 1.6×10^6 cells (mean: 62,7×10^6 cells). For the patients of cohort 4 the yield of CD141 (BDCA-3)$^+$ cells varied between 3.2 and 8.0 × 10^6 cells (mean: 5.0×10^6 cells). After the processing steps (depletion of CD14$^+$ and CD19$^+$ cells, enrichment of myDCs and volume reduction of the selected cells suspensions) the number of CD1c (BDCA-1)$^+$ cells varied among all cohorts between 13.7 and 36.9 × 10^6 cells (mean: 22.0×10^6 cells), excluding the outlier of cohort 1 with a lower yield of 0.25×10^6 cells. The purity of CD1c (BDCA-1)$^+$ myDCs varied between 80.8 and 89.8% (mean: 85.3 %) for cohorts 1/2/3 (excluding the outlier of cohort 1 with a purity of 26.2%) (online supplemental table S1). For patients of cohort 4, processing resulted in a final cell purity that varied for CD1c (BDCA-1)$^+$ myDCs between 51.7% and 66.7% (mean: 60.9 %) and for CD141 (BDCA-3)$^+$ myDCs between 3.4% and 9.4% (mean 5.8%). In this last cohort, all enriched myDCs were used for infusion, with CD1c (BDCA-1)$^+$ / CD141 (BDCA-3)$^+$ myDC numbers varying between 15.6 and 40.0 × 10^6, with a mean of 28.8×10^6 myDCs (online supplemental table S1). For all processed cell suspensions, the nucleated cell viability at time of injection varied between 82.0 and 99.6% (mean: 97.1%).

Treatment disposition

All 13 patients were injected with the predefined dose of myDCs and were evaluated for toxicity. In cohort 1, one patient was treated with 0.5×10^6 CD1c (BDCA-1)$^+$ myDCs, a second patient was treated with 0.25×10^6 CD1c (BDCA-1)$^+$ myDCs due to a low yield. In cohort 2, two patients were treated with 1×10^6 CD1c (BDCA-1)$^+$ myDCs. In cohort 3, three patients were treated with 10×10^6 CD1c (BDCA-1)$^+$ myDCs. Six patients in cohort 4 received all isolated CD1c (BDCA-1)$^+$ / CD141 (BDCA-3)$^+$ myDCs. At baseline, a median number of two lesions (range 1–15) was injected. Injected metastases included metastases to the skin (n=7), lymph node metastases (n=4), and other soft tissue metastases (n=2). The total amount of myDCs was distributed between the different lesions that were selected to be injected beforehand and were injected with T-VEC the day before. The total number of T-VEC administrations was a median of 6 (range 3–8).

Safety and AEs

Most treatment-related AEs (TRAEs) were low grade in severity and were self-limiting or manageable with supportive medication. We most frequently observed constitutional AEs, including fatigue in 11 patients (85%; of which 2 patients (15%) with grade 3 fatigue), fever in eight patients (62%), chills and other influenza-like symptoms in six patients (46%). Nine patients (69%) experienced injection-site pain, four patients (31%) had redness of injected lesion(s). Patients also reported gastrointestinal symptoms including nausea (n=8; 62%) and abdominal pain (n=5; 39%).

In cohort 4, one patient was hospitalized due to a grade 3 inflammatory reaction with an acute decline in kidney function and transient liver enzyme elevation, which spontaneously resolved within 24 hours. In cohort 3, one

Table 2 Treatment-related adverse events (N=13)

	All cohorts			
Adverse event	All grades N (%)	Grade 1 N (%)	Grade 2 N (%)	Grade ≥3 n (%)
Fatigue	11 (85)	5 (39)	4 (31)	2 (15)
Injection-site pain	9 (69)	7 (54)	2 (15)	-
Fever	8 (62)	5 (39)	3 (23)	-
Nausea	8 (62)	7 (54)	–	1 (8)
Chills	6 (46)	3 (23)	3 (23)	-
Influenza-like symptoms	6 (46)	5 (39)	1 (8)	-
Abdominal pain	5 (39)	5 (39)	-	-
Redness at injection-site	4 (31)	4 (31)	–	-
Headache	4 (31)	3 (23)	1 (8)	–
Myalgia	3 (23)	3 (23)	–	-
Malaise	3 (23)	3 (23)	–	–
Pruritus (generalized)	3 (23)	2 (15)	1 (8)	–
Transpiration	3 (23)	1 (8)	2 (15)	–
Diarrhea	3 (23)	3 (23)	–	–
Inflammatory syndrome	2 (15)	–	1 (8)	1 (8)
Hyperkalemia	2 (15)	2 (15)	–	–
Liver enzyme elevation	2 (15)	2 (15)	–	–
Eosinophilia	1 (8)	–	–	1 (8)
Purpuric rash	1 (8)	1 (8)	–	-
Arterial hypertension	1 (8)	–	–	1 (8)
Blurry vision	1 (8)	1 (8)	–	-
Acute kidney injury	1 (8)	–	–	1 (8)
Pruritus (localized)	1 (8)	1 (8)	–	–
Local hemorrhage	1 (8)	1 (8)	–	–
Vertigo	1 (8)	1 (8)	–	–
Rash (local)	1 (8)	1 (8)	–	–
Hematoma (local)	1 (8)	1 (8)	–	–
Inflammation/hemorrhage (local)	1 (8)	1 (8)	–	–
Photophobia	1 (8)	1 (8)	–	–

patient developed an asymptomatic grade 3 blood eosinophilia which persisted during the whole treatment but returned to baseline levels after stopping the treatment on achieving a pathologically confirmed complete response (CR) (online supplemental figure S2A,B). The second patient in cohort 3 who obtained a CR developed a grade 1 purpuric rash in the area of injected metastatic lesions 2 days after injection of CD1c (BDCA-1)$^+$ myDCs that resolved completely after approximately 7 days without any therapeutic intervention (online supplemental figure S2C). No grade 4 or 5 AE was reported. An overview of all TRAE is provided in table 2.

Clinical outcome

At the time of analysis, five patients were alive, and eight patients had died due to melanoma. Twelve patients (92%) were evaluable for tumor response by ^{18F}FDG PET/CT assessment following 12 weeks of study treatment; study treatment was stopped at an earlier point in one patient in cohort 1 due to rapid disease progression.

We observed clinical responses in injected as well as non-injected metastases; in three patients (23%) a CR of injected lesions was observed, a partial response (PR) in three patients (23%), and stable disease (SD) in two patients (15%). In five patients (39%), the injected metastases progressed on treatment. The best overall response according to iRECIST was a CR in two patients (15%), an unconfirmed PR in one patient (8%), and PD in nine patients (69%). In two patients (15%) with PD according to iRECIST, a mixed response was observed with durable complete regression of injected and non-injected metastases while progressing of other lesions and developing new lesions. Duration of response per individual patient is depicted in figure 2. An overview of clinical outcome

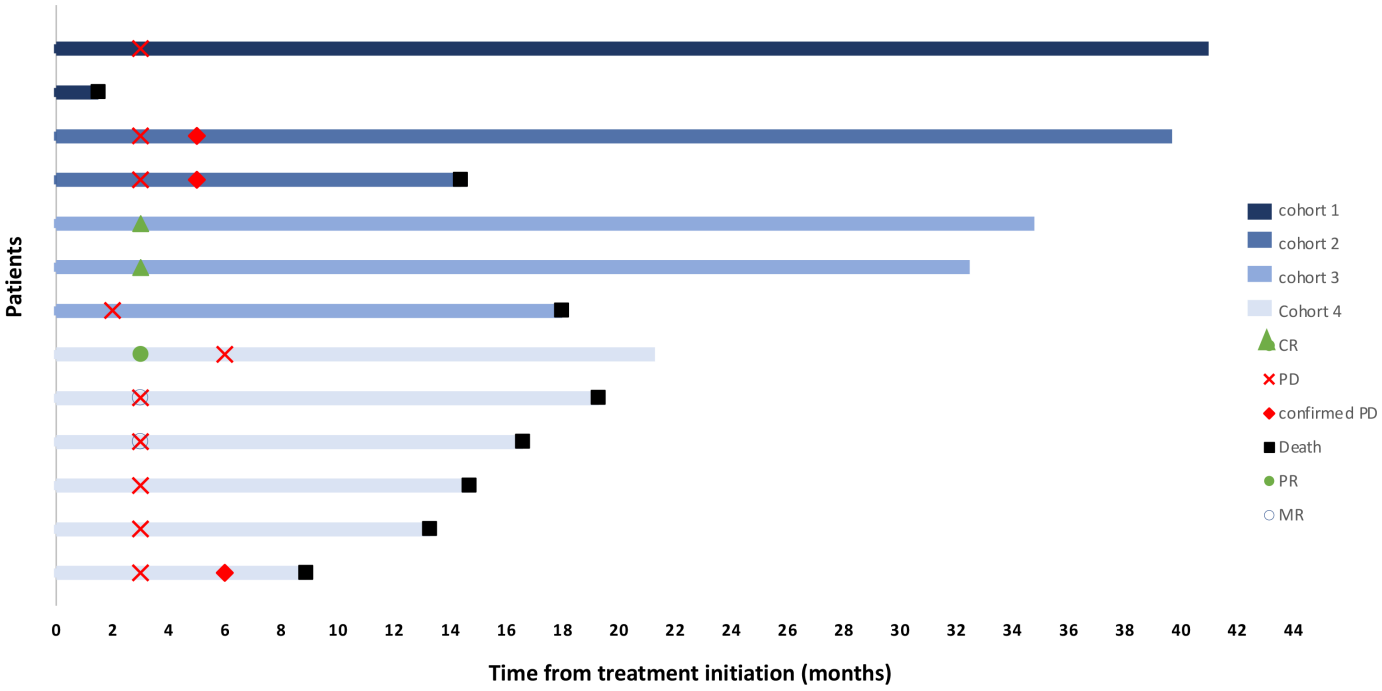

Figure 2 Kinetics of responses. Swimmer plot representing the response kinetics and duration of response (in months) of the individual patients (n=13) according to iRECIST. Green triangle, green dot, red cross, red cube, circle, black square respectively depicts complete remission (CR), partial remission (PR), progressive disease (PD), confirmed PD, mixed response (MR), and depicts death. At the time of data cut-off, CR was ongoing in two patients of cohort 3. iRECIST, Response Evaluation Criteria in Solid Tumors for immunotherapy.

per individual patient is listed in online supplemental table S1.

Two patients (29%) treated in cohort 3 obtained a CR. One patient with stage IIIC BRAF-mutant melanoma who previously progressed on anti-PD-1 therapy had multiple subcutaneous in-transit metastases on her right upper thigh of which five selected lesions were injected with myDCs (figure 3). The CR was pathologically confirmed, and the patient has an ongoing CR at 35 months following study treatment initiation. A second patient with stage IV-M1a melanoma who previously was treated with anti-PD-1 and anti-CTLA-4 therapy achieved a CR that was pathologically confirmed and eventually lead to treatment discontinuation. The patient remains in CR 33 weeks after initiating study treatment. In both patients, tumor regression became clinically evident approximately three weeks after injection of the myDCs.

One patient with stage IV-M1d disease had an unconfirmed PR at the first tumor response assessment 12 weeks after initiating study treatment. After one single subcutaneous lesion was initially injected with myDCs, the injected as well as non-injected distant lymph node lesions decreased in volume and metabolic activity. Another subcutaneous lesion was then injected with T-VEC. At subsequent tumor response assessment 12 weeks later, all known lesions (injected as well as non-injected lesions) again had increased in volume and metabolic activity.

One patient with stage IV-M1c BRAF-wild-type melanoma with multiple in-transit metastases on his left leg, lung metastases, and a cardiac metastasis achieved a CR of all in-transit metastases (injected as well as non-injected metastases). Lung metastases and the cardiac metastasis remained stable. However, the patient developed a new pathological lymph node metastasis in the head and neck region. This metastasis was subsequently injected with T-VEC for three cycles which did not result in a clinical response and led to clinical symptoms for which radiotherapy was administered.

Tissue analysis

Longitudinal core needle biopsies were performed in eight (62%) patients. HE-staining and basic IHC for $CD3^+$, $CD8^+$ cells, and PD-L1 expression was performed on all tissue samples; an 8-plex immunofluorescent staining for CD3, CD4, CD8, CD68, FoxP3, PD-1, PD-L1, and SOX10 was performed on selected baseline and on-treatment biopsies from five patients.

In both patients who obtained a CR, an increase in immune cell infiltrate was evident on HE-staining and IHC. In one patient (cohort 3) who initially had multiple in-transit lesions on her right upper thigh (figure 3A), only a few tumor infiltrating lymphocytes were present at baseline as shown by IHC, with subsequent increasing infiltration during study treatment (figure 3B). mIF analysis confirmed a significant increase in CTL in both tumor and non-tumor areas and decreased densities in exhausted T cells ($CD3^+$ $PD\text{-}1^+$ cells) (figure 3C,D). Furthermore, densities of tumor-associated macrophages (TAM), both M1-like ($CD68^+$ $PD\text{-}L1^-$) and immunosuppressive

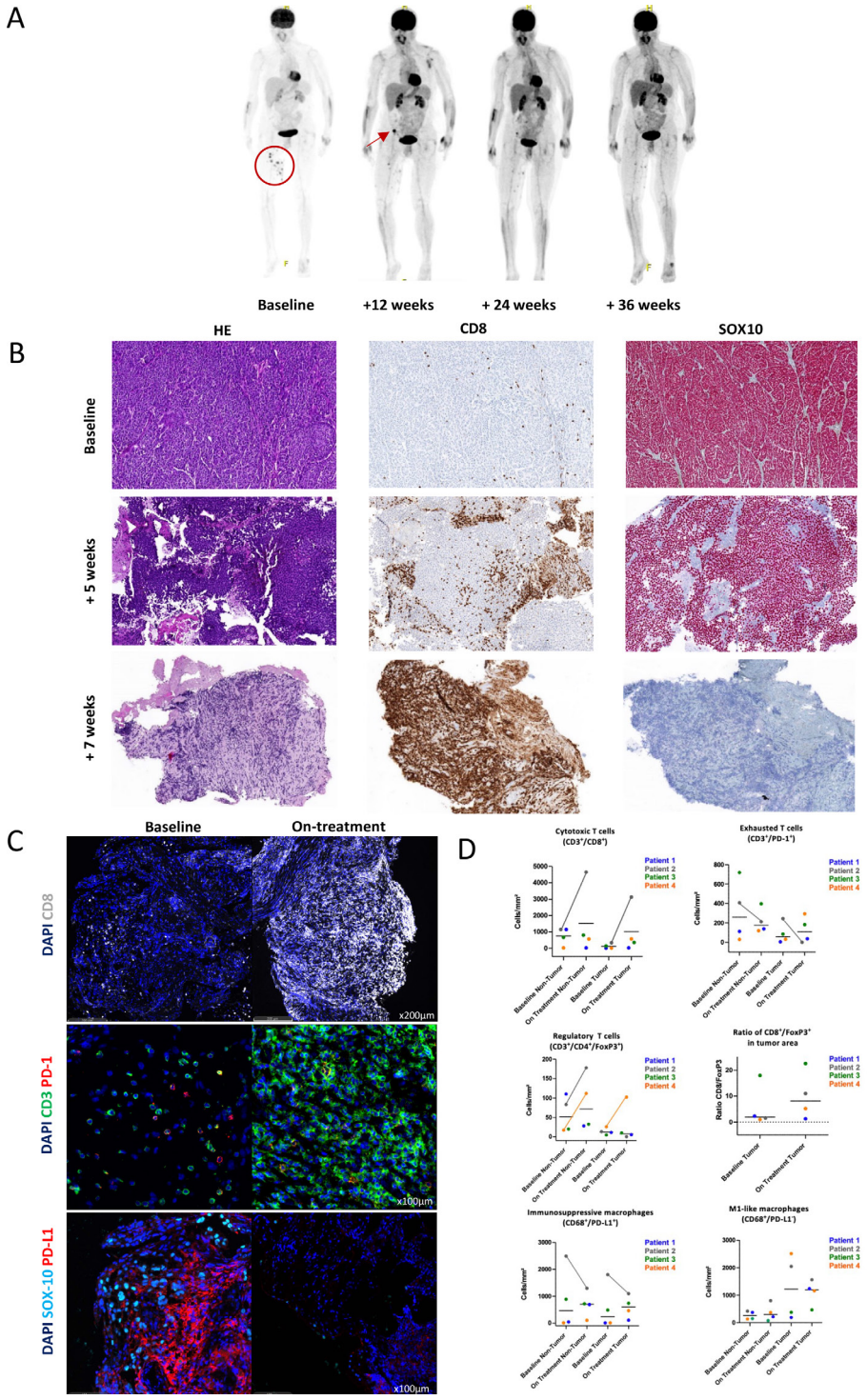

Figure 3 Case illustration of a patients who achieved a complete remission and baseline and on-treatment cell densities. (A) Tumor response on ^{18F}FDG PET/CT of a female patient in her late 60s with stage IIIC melanoma at baseline, +12 weeks, +24 weeks, and +36 weeks from baseline. While the subcutaneous lesions on the right upper thigh (red circle) decreased at 12 weeks, a new metabolically active inguinal lymph node appeared (red arrow) which then decreased in volume spontaneously on subsequent imaging. (B) Time series of representative HE and immunohistochemical (CD8, SOX10) images of tissue biopsies of injected lesions at baseline, at 5 weeks (after two treatment administrations), at 7 weeks (confirming pathological response). (C) Multiplexed immunofluorescence images (markers included CD3, CD4, CD8, CD68, FoxP3, PD-1, PD-L1, panCK/SOX10, and DAPI as nuclear counterstain) of a tissue biopsy was performed at baseline and at 7 weeks. The upper panels show an overlay of DAPI and CD8; the middle panels an overlay of DAPI, CD3 and PD-1; and the lower panels shows an overlay of DAPI, SOX-10 and PD-L1. Images were scanned at a magnification of 200 µm. (D) Cell densities (cells/mm^2), calculated from the multiplex IHC images, of cytotoxic T cells (CD3$^+$ CD8$^+$ cells), exhausted T cells (CD3$^+$ PD-1$^+$ cells), regulatory T cells (FoxP3$^+$ CD4$^+$ cells), immunosuppressive (CD68$^+$ PD-L1$^+$ cells) and M1-like macrophages (CD68$^+$ cells), and the ratio of CD3$^+$/FoxP3$^+$ cells in the tumor area. ^{18F}FDG PET/CT, (18F) positron emission tomography-CT.

macrophages (CD68$^+$ PD-L1$^+$) decreased for this patient (figure 3C,D).

In the second patient with CR, initially a T-cell excluded phenotype was observed and the number of infiltrating CD8$^+$ T cells increased subsequently. Treatment initiation in this patient was accompanied by an exponential increase in blood eosinophils and, interestingly, eosinophils infiltrating the skin on the biopsy pathologically confirming the CR were observed.

In one patient with in-transit lesions on his left leg of which selected lesions were initially injected with CD1c (BDCA-1)$^+$ / CD141 (BDCA-3)$^+$ myDC repetitive biopsies of injected as well as non-injected lesions revealed high infiltration of CD8$^+$ T cells, whereas baseline biopsy showed no significant infiltration of lymphocytes, but only sporadic lymphocytes present. Eventually, this patient developed a new lymph node metastasis in his neck not responding on intratumoral injections of T-VEC. mIF analysis of tumor biopsies of this patient confirmed the increase in CTL as well as exhausted T cells in the tumor as well as non-tumor areas. There was also an important increase in density of regulatory T cells (Tregs). In addition, densities of TAM showed likewise an increase.

Baseline biopsies of patients who had PD showed only a few solitary lymphocytes and absent PD-L1 expression on IHC which did not increase on repetitive injections. mIF analysis of tumor biopsies of one patient with PD (patient 1) confirmed no increase in CTL or exhausted T cells in the tumor areas (figure 3D). There was also no increase in Tregs or immunosuppressive macrophages in this patient (figure 3D).

An increased density of Tregs was observed in responders which was accompanied by an increase in CTL infiltration as implicated by an increased CD8$^+$ T cells/Treg ratio. Patients who had PD did not show increased densities in Tregs (figure 3D).

We performed GEP of bulk tumor tissue from nine tumor biopsies. We compared pretreatment samples and on-treatment samples from four patients (for one patient only an on-treatment sample was available). We investigated all available IO360 gene signatures (unsupervised hierarchical clustering of IO360 signatures for each sample is represented in figure 4A). We observed a significant upregulation of genes related to following signatures: PD-1 (p=0.001552), CD8$^+$ T cells (p=0.002307), T cells (p=0.007431), cytotoxic cells (p=0.001873), cytotoxicity (p=0.00414), B cells (p=0.003811), NK cells (p=0.003297), IDO1 (p=0.01158), CD45 (p=0.01659), NK CD56dim (p=0.01108), tumor inflammation signature (TIS)[42] (p=0.02131), lymphoid signature (p=0.009442), exhausted CD8 (p=0.01614), PD-L1 (p=0.03382), inflammatory chemokines (p=0.02199), PD-L2 (p=0.02745), and IL10 (p=0.02297) (figure 4B,C). No difference in GEP profile was observed between patients with PD and the patient with CR. Patient myDCTV-12 in this GEP profiling showed regression in injected lesions, while the OR of this patient was PD. The biopsies from this patient were taken from a regressing lesion, where we noted an inflamed TME, although accompanied with tolerogenic signatures. Interestingly, in one patient (myDCTV-09) who had PD we observed a downregulation in genes clustering in the antigen-presenting machinery, suggestive of β2-microglobulin-loss.

DISCUSSION

This exploratory phase I trial demonstrates that it is feasible and safe to perform intratumoral coinjection of autologous, non-substantially manipulated CD1c (BDCA-1)$^+$ myDCs with or without CD141 (BDCA-3)$^+$ myDCs in combination with T-VEC in patients with ICB-refractory melanoma. All enrolled patients successfully underwent a leukapheresis and received the predefined dose of myDCs. Patients developed mainly low-grade TRAE that were self-limiting or improved with supportive treatment and were also known to occur with T-VEC monotherapy, except for a purpuric rash and eosinophilia. Eosinophils have been associated with both protumoral and antitumoral properties.[43] In our case, we speculate that the CD1c (BDCA-1)$^+$ myDCs plus T-VEC elicited a strong immune response in which eosinophils were involved that potentially helped to eradicate the melanoma cells, especially since eosinophils were found within the TME at the time of tumor regression. Moreover, blood eosinophilia has been correlated with better outcomes to ICB.[44] In a second complete responder, transient FDG-uptake in a draining pelvic lymph node illustrates the strength of the antitumor immune response and represents a challenge in discriminating this new hot spot from distant tumor progression. Of interest, CR of clinically visible lesions that were observed in these two patients were fast (observed within 7–9 weeks following the initiation of study treatment), and durable, lasting for almost 3 years and ongoing at time of analysis. Clinical responses were observed in injected as well as non-injected lesions. Histopathological examination of on-treatment tumor biopsies is suggestive of a reinvigorated antitumor immune response.

The remarkable advances in effective T-cell-centered cancer immunotherapy that were achieved by blocking the PD-1/PD-L1/-L2 immune checkpoint axis are believed to rely on the pre-existence of an effective cancer-immunity cycle where eradication of the tumor cells is solely restricted by this inhibitory immune checkpoint signaling.[45] For any of these established ICB therapies to be successful, there needs to be an initial phase of immune recognition of the cancer cells and subsequently antitumor T cells need to be able to gain access to and exert their function within the TME. A critical role in the initiation of antigen-specific antitumor immunity and in the relicensing of antitumor T-cell function within the TME has been attributed to myDCs. Taking into account that migration of myDCs from the blood to the TME, subsequent maturation, and trafficking to lymphoid structures are likely to be defective or absent in ICB-refractory melanoma,

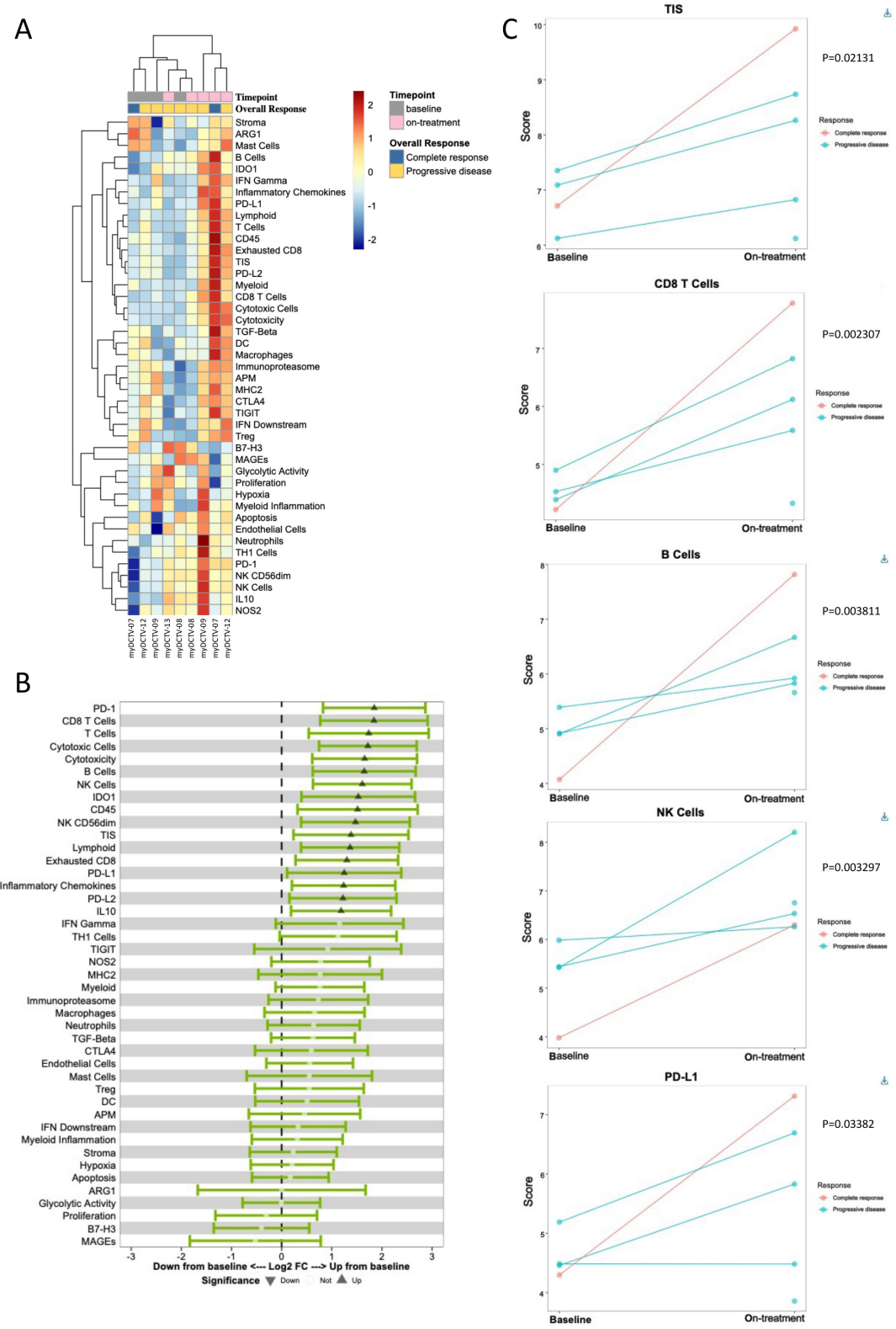

Figure 4 Gene expression profiling of baseline and on-treatment biopsies. (A) Heat map representing unsupervised hierarchical clustering of signature scores (each vertical line represents the scores for one sample). Scores are scaled by signature to have a mean of zero and a SD of one. The color code indicates the relative value of signature score, and the color key is shown on the right. For four patients, a baseline and an on-treatment biopsy were analyzed, for one patient only an on-treatment sample was analyzed (sample annotations are depicted on top of the heatmap). (B) Forest plot showing the differential expression means and 95% CI between two time points for each level of a secondary grouping variable, for each signature on an unadjusted scale. Triangles show significantly upregulated signatures while open circles indicate non-significantly changed signatures. (C) Time series of baseline and on-treatment biopsies. Spaghetti plots displaying individual sample scores for a single signature ($CD8^+$ T cells, B cells, NK cells, TIS, PD-L1). NK, natural killer.

we sought to reinvigorate the cancer-immunity cycle by reconstituting the intratumoral presence of CD1c (BDCA-1)$^+$ / CD141 (BDCA-3)$^+$ myDCs through intratumoral injection. T-VEC was coinjected to increase the amount of available tumor antigens and to optimize the potential for CD1c (BDCA-1)$^+$ / CD141 (BDCA-3)$^+$ myDC-maturation in situ. We have shown in preclinical experiments that T-VEC is non-toxic for human CD1c (BDCA-1)$^+$ myDCs and CD141 (BDCA-3)$^+$ myDCs, and provides a maturation signal leading to partial myDC maturation and the ability of cross-presentation of tumor antigens from melanoma cell lines treated with T-VEC.[46] Functional experiments have shown that T-VEC and supernatant from T-VEC-treated melanoma cell lines induces cytokine secretion in CD1c (BDCA-1)$^+$ myDCs and CD141 (BDCA-3)$^+$ myDCs.

Real-life experience with T-VEC in patients with advanced melanoma has largely been limited to treatment-naive patients; best ORR was 88.5% with a best CR rate of 61.5% for injected lesions.[47] In contrast, all patients in our clinical trial were heavily pretreated with multiple lines of treatment. We reported earlier on two patients who achieved a PR on treatment with T-VEC while previously progressing on ICB.[48] We therefore cannot completely exclude that the two CR obtained in this limited series of 13 patients could have been achieved with T-VEC monotherapy. The fast kinetics and depth of response, however, seem superior to our previously reported cases. Moreover, the atypical hemorrhagic rash with associated tumor response as well as the blood eosinophilia, both not known to have been reported in relation with T-VEC monotherapy, suggest an additional effect of the intratumorally administered myDCs.

Unfortunately, patients with a higher tumor burden and hematogenic metastases did not respond sufficiently well to the treatment, obtaining SD or PR in injected lesions but overall PD. Addressing the differences between responding cutaneous metastases and non-responding visceral metastases, therefore, could represent an opportunity to address mechanisms of resistance, be it tumor cell intrinsic or related to dysfunction of immune cells within the specific TME.

On-treatment biopsies revealed increasing T-lymphocyte infiltration in patients with CR already in the early course of the treatment. In addition, GEP revealed upregulations in gene signatures related to antitumor immunity (eg, TIS). Information from repetitive biopsies could serve as a biomarker for intratumoral treatment strategies. Longitudinal tumor samples have been evaluated as a biomarker of response or to find mechanisms of treatment-resistance in a cohort of melanoma patients under ICB.[49] It has been shown that signatures of an adaptive immune response on early tumor samples were highly predictive of response to the treatment. Tumor response assessment by ^{18F}FDG-PET/CT may underestimate tumor responses, leading to confounding observations of pseudoprogression in stimulated lymph nodes. In this case, tumor biopsies can be of added value to assess intralesional changes. In contrast, in patients whose tumor biopsies do not show an increase in infiltrating T lymphocytes or upregulation of PD-L1 could serve for studying mechanisms of resistance and guide future therapeutic decisions.

DC-based vaccines, predominantly with ex vivo-cultured monocyte-derived DC (moDCs), have shown antitumor activity in various solid tumors. However, clinical responses were highly variable. Due to a higher functional specialization, naturally circulating DC (nDC) possess better antigen-presenting capacities compared with moDCs.[24] Our clinical trial is the first worldwide that investigates the intratumoral administration of CD1c (BDCA-1)$^+$/CD141 (BDCA-3)$^+$ myDCs without any substantial ex vivo manipulation. nDCs, both myDCs and pDCs alone or in combination, have been or are currently under investigation as a 'classical' DC-vaccine in several studies. Treatment with myDC-vaccines in melanoma patients or vaccination with the combination with myDCs and pDCs in patients with prostate cancer have shown encouraging results.[29 30] However, our intratumoral 'antigen agnostic' approach may be advantageous in exploiting the full potential of generating immune responses against private neoantigens. T-VEC may prevent intratumorally injected myDCs to immediately develop a tolerogenic character within the immunosuppressive TME. DC-vaccines comprise complex ex vivo conditions and the necessity of an advanced therapy medicinal product (ATMP)-facility implicating much higher production costs. The use of intratumorally injected, non-substantially manipulated CD1c (BDCA-1)$^+$ myDCs and CD141 (BDCA-3)$^+$ myDCs has been classified as a non-ATMP by the European Committee for Advanced Therapies and could consequently easily be implemented in institutions with more limited infrastructure.

CONCLUSIONS

In conclusion, intratumoral injection of autologous CD1c (BDCA-1)$^+$ myDCs with or without CD141 (BDCA-3)$^+$ myDCs in combination with intratumoral coinjection of T-VEC is feasible and tolerable. This treatment regimen resulted in encouraging signs of antitumor activity in pretreated melanoma patients with two patients developing a durable CR legitimating further evaluation.

Author affiliations
[1]Department of Medical Oncology/Laboratory of Medical and Molecular Oncology (LMMO), Vrije Universiteit Brussel (VUB), Universitair Ziekenhuis Brussel (UZ Brussel), Brussels, Belgium
[2]Department of Anatomopathology, Vrije Universiteit Brussel (VUB), Universitair Ziekenhuis Brussel (UZ Brussel), Brussels, Belgium
[3]Ultivue, Inc, Cambridge, Massachusetts, USA
[4]Department of Radiotherapy, Vrije Universiteit Brussel (VUB), Universitair Ziekenhuis Brussel (UZ Brussel), Brussels, Belgium
[5]Stem Cell Laboratory, Department of Hematology, Vrije Universiteit Brussel (VUB), Universitair Ziekenhuis Brussel (UZ Brussel), Brussels, Belgium

Acknowledgements The authors would like to thank the patients and their families who enrolled on this clinical trial, along with the clinical research staff. The authors also would like to thank Khrystyna North from NanoString for her valuable help. This research has been resented in part at the 34th Annual meeting of the Society of Immunotherapy for Cancer, November 6, 2019–November 10, 2019, National Harbor, MD, USA, and at the European Society of Medical Oncology Congress 2021 in Paris, France.

Contributors JKS and BN drafted the clinical trial protocol. JKS conducted acquisition, analysis, and interpretation of the data. JKS, JT, GA and BN provided care for patients. JKS, JT and BN administered study treatment. IVR was responsible for cell isolation and preparation of the final cell product. JKS, LC, RF, AV, CB and ID performed tissue analysis. JKS wrote and edited the manuscript under supervision of BN. BN is responsible for the overall content as guarantor. All authors reviewed the manuscript. Final manuscript was read and approved for submission by all authors.

Funding The research in this manuscript is funded by Kom op tegen Kanker (Stand up to Cancer), the Flemish cancer society (reference No 11102), and Stichting tegen Kanker. Final manuscript writing was supported by Oncology Center Vrije Universiteit Brussel. Talimogene laherparepvec (T-VEC) was provided by Amgen.

Competing interests JKS reports non-financial support from MSD and Amgen; personal fees from Novartis. GA reports grants and nonfinancial support from Pfizer, Novartis; nonfinancial support from MSD, Astellas; personal fees from Novartis, Biocartis. BN reports personal financial compensation from Roche, Bristol-Myers Squibb, Merck Sharp & Dohme, Novartis, AstraZeneca for public speaking, consultancy, and participation in advisory board meeting. The institution (UZ Brussel) received research funding related to research projects conducted by Bart Neyns from Pfizer, Novartis, Roche, Merck-Serono. The other authors do not declare any competing interests.

Patient consent for publication Consent obtained directly from patient(s).

Ethics approval This study involves human participants and was approved by Medical ethics committee of Universitair Ziekenhuis Brussel (2018/047). Participants gave informed consent to participate in the study before taking part.

Provenance and peer review Not commissioned; externally peer reviewed.

Data availability statement Data are available on reasonable request. The datasets used and/or analyzed during the current study are available from the corresponding author on reasonable request.

ORCID iDs
Julia Katharina Schwarze http://orcid.org/0000-0001-8990-5380
Gil Awada http://orcid.org/0000-0001-9535-0430
Bart Neyns http://orcid.org/0000-0003-0658-5903

REFERENCES

1 Robert C, Ribas A, Schachter J, *et al*. Pembrolizumab versus ipilimumab in advanced melanoma (KEYNOTE-006): post-hoc 5-year results from an open-label, multicentre, randomised, controlled, phase 3 study. *Lancet Oncol* 2019;20:1239–51.
2 Wolchok JD, Chiarion-Sileni V, Gonzalez R, *et al*. Overall survival with combined nivolumab and ipilimumab in advanced melanoma. *N Engl J Med* 2017;377:1345–56.
3 Larkin J, Chiarion-Sileni V, Gonzalez R, *et al*. Combined nivolumab and ipilimumab or monotherapy in untreated melanoma. *N Engl J Med* 2015;373:23–34.
4 Hodi FS, O'Day SJ, McDermott DF, *et al*. Improved survival with ipilimumab in patients with metastatic melanoma. *N Engl J Med* 2010;363:711–23.
5 Postow MA, Chesney J, Pavlick AC, *et al*. Nivolumab and ipilimumab versus ipilimumab in untreated melanoma. *N Engl J Med* 2015;372:2006–17.
6 Larkin J, Chiarion-Sileni V, Gonzalez R, *et al*. Five-year survival with combined nivolumab and ipilimumab in advanced melanoma. *N Engl J Med* 2019;381:1535–46.
7 Robert C, Grob JJ, Stroyakovskiy D, *et al*. Five-year outcomes with dabrafenib plus trametinib in metastatic melanoma. *N Engl J Med* 2019;381:626–36.
8 Chen DS, Mellman I. Oncology meets immunology: the cancer-immunity cycle. *Immunity* 2013;39:1–10.
9 Chen DS, Mellman I. Elements of cancer immunity and the cancer-immune set point. *Nature* 2017;541:321–30.
10 Mellman I. Dendritic cells: master regulators of the immune response. *Cancer Immunol Res* 2013;1:145–9.
11 Broz ML, Binnewies M, Boldajipour B, *et al*. Dissecting the tumor myeloid compartment reveals rare activating antigen-presenting cells critical for T cell immunity. *Cancer Cell* 2014;26:638–52.
12 Roberts EW, Broz ML, Binnewies M, *et al*. Critical Role for CD103(+)/CD141(+) Dendritic Cells Bearing CCR7 for Tumor Antigen Trafficking and Priming of T Cell Immunity in Melanoma. *Cancer Cell* 2016;30:324–36.
13 Spranger S, Dai D, Horton B, *et al*. Tumor-Residing Batf3 dendritic cells are required for effector T cell trafficking and adoptive T cell therapy. *Cancer Cell* 2017;31:711–23.
14 Binnewies M, Mujal AM, Pollack JL, *et al*. Unleashing Type-2 Dendritic Cells to Drive Protective Antitumor $CD4^+$ T Cell Immunity. *Cell* 2019;177:556–71.
15 Laoui D, Keirsse J, Morias Y, *et al*. The tumour microenvironment harbours ontogenically distinct dendritic cell populations with opposing effects on tumour immunity. *Nat Commun* 2016;7:13720.
16 Spranger S, Gajewski TF. A new paradigm for tumor immune escape: β-catenin-driven immune exclusion. *J Immunother Cancer* 2015;3:43.
17 Spranger S, Bao R, Gajewski TF. Melanoma-intrinsic β-catenin signalling prevents anti-tumour immunity. *Nature* 2015;523:231–5.
18 Salmon H, Idoyaga J, Rahman A, *et al*. Expansion and Activation of CD103(+) Dendritic Cell Progenitors at the Tumor Site Enhances Tumor Responses to Therapeutic PD-L1 and BRAF Inhibition. *Immunity* 2016;44:924–38.
19 Böttcher JP, Bonavita E, Chakravarty P, *et al*. Nk cells stimulate recruitment of cdc1 into the tumor microenvironment promoting cancer immune control. *Cell* 2018;172:1022–37.
20 Spranger S, Luke JJ, Bao R, *et al*. Density of immunogenic antigens does not explain the presence or absence of the T-cell-inflamed tumor microenvironment in melanoma. *Proc Natl Acad Sci U S A* 2016;113:E7759–68.
21 Barry KC, Hsu J, Broz ML, *et al*. A natural killer-dendritic cell axis defines checkpoint therapy-responsive tumor microenvironments. *Nat Med* 2018;24:1178–91.
22 Garris CS, Arlauckas SP, Kohler RH, *et al*. Successful anti-PD-1 cancer immunotherapy requires T Cell-Dendritic cell crosstalk involving the cytokines IFN-γ and IL-12. *Immunity* 2018;49:1148–61.
23 Villani A-C, Satija R, Reynolds G, *et al*. Single-cell RNA-seq reveals new types of human blood dendritic cells, monocytes, and progenitors. *Science* 2017;356. doi:10.1126/science.aah4573. [Epub ahead of print: 21 04 2017].
24 Bol KF, Schreibelt G, Rabold K, *et al*. The clinical application of cancer immunotherapy based on naturally circulating dendritic cells. *J Immunother Cancer* 2019;7:109.
25 Di Blasio S, Wortel IMN, van Bladel DAG, *et al*. Human CD1c(+) DCs are critical cellular mediators of immune responses induced by immunogenic cell death. *Oncoimmunology* 2016;5:e1192739.
26 Nizzoli G, Krietsch J, Weick A, *et al*. Human CD1c+ dendritic cells secrete high levels of IL-12 and potently prime cytotoxic T-cell responses. *Blood* 2013;122:932–42.
27 Sköld AE, van Beek JJP, Sittig SP, *et al*. Protamine-stabilized RNA as an ex vivo stimulant of primary human dendritic cell subsets. *Cancer Immunol Immunother* 2015;64:1461–73.
28 Tel J, Aarntzen EHJG, Baba T, *et al*. Natural human plasmacytoid dendritic cells induce antigen-specific T-cell responses in melanoma patients. *Cancer Res* 2013;73:1063–75.
29 Westdorp H, Creemers JHA, van Oort IM, *et al*. Blood-derived dendritic cell vaccinations induce immune responses that correlate with clinical outcome in patients with chemo-naive castration-resistant prostate cancer. *J Immunother Cancer* 2019;7:302.
30 Schreibelt G, Bol KF, Westdorp H, *et al*. Effective clinical responses in metastatic melanoma patients after vaccination with primary myeloid dendritic cells. *Clin Cancer Res* 2016;22:2155–66.
31 Schwarze JK, Awada G, Cras L, *et al*. Intratumoral Combinatorial Administration of CD1c $(BDCA\text{-}1)^+$ Myeloid Dendritic Cells Plus Ipilimumab and Avelumab in Combination with Intravenous Low-Dose Nivolumab in Patients with Advanced Solid Tumors: A Phase IB Clinical Trial. *Vaccines* 2020;8. doi:10.3390/vaccines8040670. [Epub ahead of print: 10 11 2020].
32 Shen Y, Nemunaitis J. Herpes simplex virus 1 (HSV-1) for cancer treatment. *Cancer Gene Ther* 2006;13:975–92.

33 Andtbacka RHI, Kaufman HL, Collichio F, *et al*. Talimogene Laherparepvec improves durable response rate in patients with advanced melanoma. *J Clin Oncol* 2015;33:2780–8.
34 Andtbacka RHI, Ross M, Puzanov I, *et al*. Patterns of clinical response with Talimogene Laherparepvec (T-VEC) in patients with melanoma treated in the OPTiM phase III clinical trial. *Ann Surg Oncol* 2016;23:4169–77.
35 Liu BL, Robinson M, Han Z-Q, *et al*. ICP34.5 deleted herpes simplex virus with enhanced oncolytic, immune stimulating, and anti-tumour properties. *Gene Ther* 2003;10:292–303.
36 Bommareddy PK, Zloza A, Rabkin SD, *et al*. Oncolytic virus immunotherapy induces immunogenic cell death and overcomes sting deficiency in melanoma. *Oncoimmunology* 2019;8:1591875.
37 Rehman H, Silk AW, Kane MP, *et al*. Into the clinic: Talimogene laherparepvec (T-VEC), a first-in-class intratumoral oncolytic viral therapy. *J Immunother Cancer* 2016;4:53.
38 Ribas A, Dummer R, Puzanov I, *et al*. Oncolytic virotherapy promotes intratumoral T cell infiltration and improves anti-PD-1 immunotherapy. *Cell* 2017;170:1109–19.
39 Gogas HJ*et al*. Abstract 1037O - MASTERKEY-265: A phase III, randomized, placebo (Pbo)-controlled study of talimogene laherparepvec (T) plus pembrolizumab (P) for unresectable stage IIIB–IVM1c melanoma (MEL). *ESMO Congress* 2021;32 (suppl_5):S867–905.
40 Gutzmer R, Harrington KJ, Hoeller C, *et al*. Practical clinical guide on the use of talimogene laherparepvec monotherapy in patients with unresectable melanoma in Europe. *Eur J Dermatol* 2018;28:736–49.
41 Vasaturo A, Galon J. Multiplexed immunohistochemistry for immune cell phenotyping, quantification and spatial distribution in situ. *Methods Enzymol* 2020;635:51–66.
42 Damotte D, Warren S, Arrondeau J, *et al*. The tumor inflammation signature (TIS) is associated with anti-PD-1 treatment benefit in the CERTIM pan-cancer cohort. *J Transl Med* 2019;17:357.
43 Simon SCS, Utikal J, Umansky V. Opposing roles of eosinophils in cancer. *Cancer Immunol Immunother* 2019;68:823–33.
44 Moreira A, Leisgang W, Schuler G, *et al*. Eosinophilic count as a biomarker for prognosis of melanoma patients and its importance in the response to immunotherapy. *Immunotherapy* 2017;9:115–21.
45 Tumeh PC, Harview CL, Yearley JH, *et al*. PD-1 blockade induces responses by inhibiting adaptive immune resistance. *Nature* 2014;515:568–71.
46 Tijtgat J, De Munck J, Dufait I, *et al*. Unraveling the Effects of a Talimogene Laherparepvec (T-VEC)-Induced Tumor Oncolysate on Myeloid Dendritic Cells. *Front Immunol* 2021;12:733506.
47 Franke V. Talimogene laherparepvec monotherapy, an elegant alternative to systemic immunotherapy for the treatment of early metastatic melanoma. *Br J Dermatol* 2019;181:20–1.
48 Seremet T, Planken S, Schwarze JK, *et al*. Successful treatment with intralesional talimogene laherparepvec in two patients with immune checkpoint inhibitor-refractory, advanced-stage melanoma. *Melanoma Res* 2019;29:85–8.
49 Chen P-L, Roh W, Reuben A, *et al*. Analysis of immune signatures in longitudinal tumor samples yields insight into biomarkers of response and mechanisms of resistance to immune checkpoint blockade. *Cancer Discov* 2016;6:827–37.